

# Direct measurement of oxygen partial pressure in a flying bumblebee

Yutaka Komai\*

*ERATO, Kawachi Millibioflight Project, Park Building, 4-7-6 Komaba, Meguro, Tokyo, Japan*

\*Present address: Department of Vascular Physiology, Research Institute, National Cardiovascular Center, 5-7-1 Fujishirodai, Suita, Osaka 565, Japan (e-mail: miesha@tani.sd.keio.ac.jp)

Accepted 13 June 2001

## Summary

The gas transport system of a bumblebee was investigated by measuring the oxygen partial pressure  $P_{O_2}$  in the wing muscle. In the resting bee,  $P_{O_2}$  showed a regular pattern of fluctuation with a typical period of 70–120 s. Fluctuations in muscular  $P_{O_2}$  were associated with intermittent abdominal pumping. Ventilation by abdominal movements may not be necessary during rest because  $P_{O_2}$  is high (8.5–9.2 kPa) in the anaesthetised bee. Thermal effects on muscular  $P_{O_2}$  were examined by cooling the bee, causing the amplitude of  $P_{O_2}$  fluctuations to increase. In most flight experiments, the bee started to fly after elevating muscle  $P_{O_2}$  by abdominal pumping;

muscle  $P_{O_2}$  then decreased at the onset of flight. However, when a flight began without pre-flight ventilation,  $P_{O_2}$  increased monotonically. During flight, muscle  $P_{O_2}$  reached a mean level ( $6.36 \pm 1.83$  kPa) that was much higher than the lowest value recorded during discontinuous ventilation during rest. The bumblebee effectively uses abdominal movements to assist in convective gas transport not only during flight but also at rest.

Key words: oxygen microelectrode, gas transport, insect, bumblebee, *Bombus hypocrita hypocruta*, flight, metabolic rate.

## Introduction

Insects use the tracheal network to supply oxygen to the tissues; this network consists of air-filled tubes (tracheae), passive diaphragms (air sacs) and valves (spiracles) (Mill, 1985). The design of the tracheal system varies dramatically among species. Mechanisms of oxygen transport also differ; for example, some aquatic insects do not have spiracles but exhibit a tracheal network in appendages that function like a fish gill (e.g. mayfly larvae, Miller, 1974). In some circumstances, insects ventilate intermittently (once an hour or less), perhaps to reduce evaporative water loss (e.g. silkworm pupae, Levy and Schneiderman, 1966).

Even in flying insects, the design of the respiratory organs and the mechanisms involved vary widely. Gas transport in the hawkmoth *Agrius convolvuli* (Komai, 1998) has been investigated previously. While diffusive gas transport supplies sufficient oxygen at rest, the moth uses convective gas transport during flight. Contraction of the flight muscle causes a ventilating air flow in the tracheae that augments gas transport to meet increased oxygen demand. For some conditions, this increased oxygen supply is more than sufficient to meet the increased demand, and the oxygen partial pressure in the flight muscle therefore increases as flight activity increases.

A foraging bumblebee has one of the highest recorded flight metabolic rates (Wolf et al., 1996). During the short rests that may follow a flight, one can observe intense pumping movements of the abdomen. The bee's abdomen is well

equipped with muscles for both contraction and extension (Snodgrass, 1984) and the bee also has well-developed air sacs in the abdomen and in the thorax. In the present study, the oxygen partial pressure,  $P_{O_2}$ , in a wing muscle of the bumblebee *Bombus hypocrita hypocruta* was measured directly using a needle electrode, and the relationship between  $P_{O_2}$  and ventilation/flight activity was investigated.

## Materials and methods

A colony of the bumblebee *Bombus hypocrita hypocruta* (L.) was obtained from Koppert Biological Systems. The bees were kept in the nest box in which the colony had been obtained, and pollen was periodically placed in the nest box. Worker bees were used in experiments ( $N=47$ ). Anatomical investigations of the thorax and muscle dimensions were carried out (as described by Komai, 1998) using frozen sections ( $N=10$ ) and dissections ( $N=10$ ). The muscle fibre diameter and the tracheole density were measured from microphotographs.

Oxygen partial pressure was measured by inserting an oxygen microelectrode directly into a thoracic flight muscle of a tethered bumblebee under a microscope. To avoid unnecessary damage to the bee, it was first anaesthetised using carbon dioxide. The hairs on the thoracic tergites were removed, and the back of the bee then was attached using adhesive (neoprene, G17, Konishe) to a stainless-steel pipe

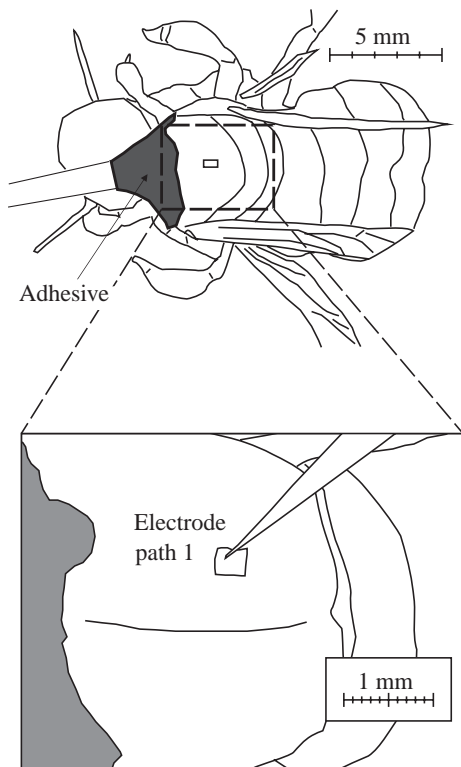
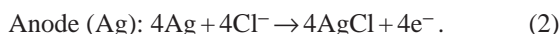


Fig. 1. Diagram of a tethered bumblebee showing the region of cuticle that was removed for electrode insertion. In this dorsal view, the tether extends to the left. In the enlarged area, the electrode is shown inserted along path 1 (see Fig. 2).

(1.3 mm in diameter) with its head downwards. The mounting pipe was connected to a metal pole and attached to a manipulator. A segment of thoracic cuticle measuring approximately  $0.3\text{ mm} \times 0.5\text{ mm}$  was removed, and the electrode was inserted through this opening into the dorsal longitudinal muscle (Fig. 1). This route of electrode insertion was termed path 1. Beneath the thoracic tergites lie air sacs and flight muscles that attach directly to the tergites, so damage to the muscle or the air sac during removal of the cuticle or insertion of the electrode was unavoidable. A second route of electrode insertion was therefore also used to investigate the effects of the opening procedure (Fig. 2). In path 1, only the muscle was potentially damaged during electrode insertion, whereas in path 2 the air sac was also punctured by the electrode. No observable differences were found between the results from the two electrode paths.

The polarographic and coaxial electrode (Pt-Ag/AgCl,  $-0.6\text{ V}$ ) had a tip diameter of  $2\text{--}8\text{ }\mu\text{m}$  (Baumgärtl, 1987). Dissolved oxygen undergoes reduction on the platinum cathode as follows:



The current produced is proportional to the oxygen partial pressure at a position just outside the recess in the electrode

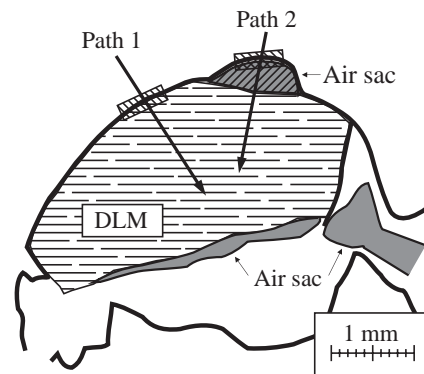


Fig. 2. Longitudinal section of the bumblebee thorax to show the two directions in which the electrodes were inserted (arrows). The hatched boxes were removed; the cuticle and muscle were removed for path 1, and the cuticle and air sac were removed for path 2. DLM, dorsal longitudinal muscle.

tip. The reduction current of the electrodes used here ranged from  $200\text{ pA}$  to  $2\text{ nA}$  in water bubbled with air and from  $2$  to  $50\text{ pA}$  in water bubbled with nitrogen. Taking into account the memory storage of the picoammeter, a sampling frequency of  $10\text{ Hz}$  and 16-bit resolution were chosen. The estimated response time of the electrode was shorter than  $0.1\text{ s}$ , so the time resolution in this measurement system was  $0.1\text{ s}$ . The electrode was calibrated in Theorel buffer (Baumgärtl, 1987) equilibrated by bubbling with gas mixtures of oxygen and nitrogen, and thermally regulated at  $30\text{ }^\circ\text{C}$ . Five-point calibrations ( $0, 5, 10, 15$  and  $20\%$   $\text{O}_2$ ) were performed three times for each experimental measurement, twice before the measurement and once after it. The mean correlation coefficient ( $r$ ) between the reduction current and the oxygen partial pressure was  $0.9984$  over 122 calibrations. The electrode surface sometimes became contaminated by tissue following an experimental measurement. In the worst case, the reduction current decreased by  $20\%$  following the measurement. Therefore, any conversion from reduction current to oxygen partial pressure was performed using the calibration curve acquired after each measurement. Room temperature was monitored using a platinum thermometer. Data from the picoammeter (M6517, Keithley Instruments) and the thermometer (M2001, Keithley Instruments) were fed into a personal computer *via* a general-purpose interface bus (GPIB). The bee was videotaped at  $30\text{ frames s}^{-1}$  using a miniature CCD camera (WV-KS152, Panasonic) for later analysis of its measurements. A time code was superimposed on the video recording by the video timer (VTG-22, For.A) to synchronize the  $P_{\text{O}_2}$  recording. Periods of flight and ventilation were identified from the wing and abdominal movements, respectively. In bees exhibiting large-amplitude abdominal ventilation, the ventilation period could be determined within an accuracy of three frames, while in bees with small, rapid abdominal movements, the period could not be determined. In flying bees with an electrode inserted along path 2, the ventilation period was determined from movements of the

exposed thoracic air sac with the same accuracy. Other details of the experimental arrangement can be found in Komai (Komai, 1998).

#### Experimental procedures

Tissue contamination decreased the sensitivity of the electrode. Such changes after electrode insertion were monitored in paralyzed bees and showed that the electrode output decreased over approximately the first 5 min following insertion and then stabilized. In all experiments, insertion at an arbitrary depth was made 10 min before a measurement to minimize the effects of this sensitivity change. Each animal was subjected to only a single insertion. Experiments were limited to 2 h because flight activity decreased over time in some bees. In this paper, a recording of one animal is termed a run.

Measurements of oxygen partial pressure were carried out at rest, during paralysis and during tethered flight. The measurement conditions for the figures are listed in Table 1. In resting experiments, 12 animals were investigated to examine the relationship between variation in  $P_{O_2}$  and ventilation behaviour. The electrode was inserted into the dorsal longitudinal muscle at four different depths (usually to 500, 1000, 1500 and 2000  $\mu\text{m}$ ) for 30 min each. If the bee struggled during insertion of the electrode, measurements were started when the bee became calm. Periods during which the bee moved its legs or wings during recording were excluded from analysis. During measurements, room temperature and ambient light intensity were kept constant. In one animal, behaviour after recovery from anaesthesia was recorded after the resting experiment; the bee was anaesthetised by placing a piece of chloroform-soaked paper near its head. In three animals, a cooling/rewarming experiment was performed after the resting measurement of 1 h; an ice pack was placed approximately 2 cm beneath the bee for 30 min and was then removed; this was repeated twice.

Twenty-five animals were used in paralysis experiments to obtain a spatial profile of  $P_{O_2}$  in the flight muscle. The bee was paralyzed by injection of 0.1 ml of  $10^{-5} \text{ mol l}^{-1}$  tetrodotoxin into the haemolymph at the neck intersegmental membrane approximately 10 min before inserting the electrode. The electrode was moved from a depth of 300  $\mu\text{m}$  to a depth of 2440  $\mu\text{m}$  in steps of 20  $\mu\text{m}$  (108 measurement points).  $P_{O_2}$  was measured for 40 s at each depth.

Ten animals were used in the flight experiments. Measurements were made at four different depths for 30 min each: 500, 1000, 1500 and 2000  $\mu\text{m}$ . When the electrode had been positioned at a particular depth, the bee was allowed to rest for 10 min and was then induced to fly (see below) four or five times. After a second 10 min rest period, a further four or five flights were recorded at the same depth. Flight was initiated by giving the bee a piece of wet tissue paper (1  $\text{cm}^2$ ) to hold with its legs. The bee rotated the tissue horizontally using its feet for several seconds, then dropped the paper and usually initiated flight for 10–15 s. The middle legs of the bee were removed for the flight experiment because flight activity

Table 1. *Experimental conditions used in the measurement of flight muscle oxygen partial pressure in bumblebees*

	Room temperature (°C)	Path	Mass (mg)	Depth ( $\mu\text{m}$ )	Condition
Run 1	28.5	1	264	750	Rest
Run 2	29.0	1	320	1000	Rest
Run 3	30.5	1	259	1500	Anaesthesia
Run 4.1	30.9	2	258	500	Cooling
Run 4.2	–	–	–	–	Rewarming
Run 5	29.1	1	NA	300–2440	Rest
Run 6	30.1	1	307	300–2440	Paralysis
Run 7	31.2	1	266	300–2440	Paralysis
Run 8	31.2	2	188	500–2000	Flight

Path, electrode path (see Fig. 2); depth, electrode depth.

was inhibited when the middle legs contacted or held the mounting arrangement.

## Results

### Resting measurements

Muscle  $P_{O_2}$  showed regular fluctuations in resting bees (Fig. 3A). The most common pattern was a triangular waveform with a rapid increase and a slower decrease in  $P_{O_2}$ . Movements of the abdomen dorsally and ventrally coincided with the increases in  $P_{O_2}$ . The mean amplitude of the  $P_{O_2}$  fluctuations was  $7.10 \pm 1.12 \text{ kPa}$  (mean  $\pm$  s.d.,  $N=12$ ) and the mean duration was  $79.0 \pm 1.6 \text{ s}$  (range 70–120 s). During the experiment shown in Fig. 3A, the bee ventilated for an average of  $8.3 \pm 1.3 \text{ s}$  during each ventilation cycle, with an abdominal pumping frequency of  $2.1 \pm 0.4 \text{ Hz}$ . The abdominal movements cause air to be moved towards the thorax from the abdomen, filling the thoracic air sacs with fresh air (Bailey, 1954). Eventually,  $P_{O_2}$  in the muscle increased. In some experiments,  $P_{O_2}$  levels fluctuated rapidly, as shown in Fig. 3B. Abdominal movements in these experiments also corresponded with increases in  $P_{O_2}$ .

Fig. 4 shows the relationship between the length of the non-ventilatory period and both the amplitude of the  $P_{O_2}$  fluctuations and the minimum values of  $P_{O_2}$ . Amplitude increased and minimum  $P_{O_2}$  decreased with increasing non-ventilatory period. Tolerance of low  $P_{O_2}$  may reduce the cost of ventilation; for example, minimum muscle  $P_{O_2}$  fell almost to zero in Fig. 3A. It is known that diffusion alone can sustain basal metabolic rate in a resting insect (Weis-Fogh, 1964). The mean  $P_{O_2}$  over a ventilation cycle varied widely from 1.78 to 7.65 kPa ( $4.88 \pm 1.45 \text{ kPa}$ , mean  $\pm$  s.d.,  $N=162$ ) and was not correlated with the length of the non-ventilatory period ( $r=-0.239$  for run 1,  $r=0.365$  for run 4,  $r=-0.738$  for run 5; all  $P>0.05$ ;  $N=49$ ,  $N=80$ ,  $N=33$  for run 1, run 4 and run 5, respectively). In some bees, mean  $P_{O_2}$  decreased as non-ventilatory period increased, but in others the opposite trend was found. This suggests that stabilization of muscle  $P_{O_2}$  is not the primary function of discontinuous ventilation.

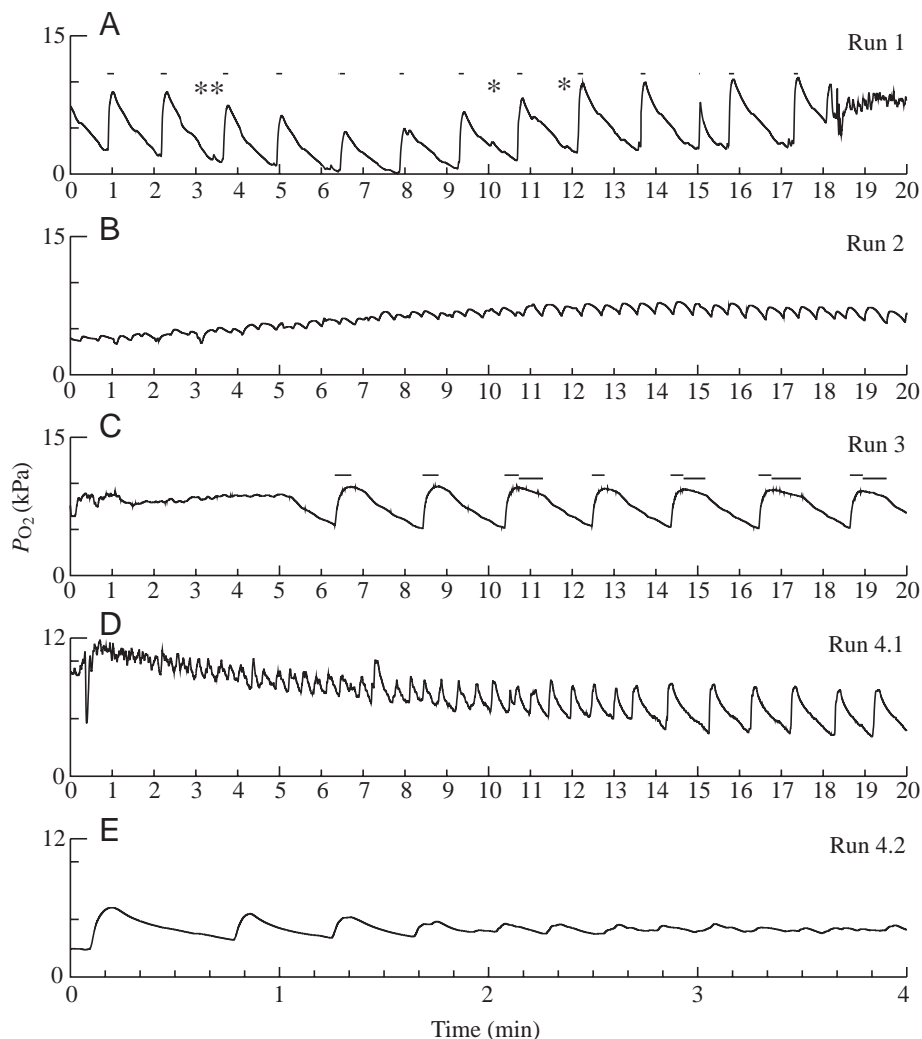


Fig. 3. Variation in flight muscle  $P_{O_2}$  in a resting bumblebee. (A) Representative pattern;  $P_{O_2}$  showed large-amplitude fluctuations. In this recording, the bee began to move its legs rapidly at 18:03 min, disrupting the regular pattern. Horizontal bars indicate periods of abdominal pumping. Asterisks indicate other abdominal movements. (B) Small-amplitude and short-interval  $P_{O_2}$  fluctuations observed under some conditions. This pattern was seen in four of the six animals when the room temperature was above 30°C and in one of the six animals when the room temperature was below 30°C. (C) Pattern recorded in a bee anaesthetised using chloroform vapour. The bee began ventilating at approximately 5 min. Thin and thick horizontal bars indicate periods of abdominal pumping and a pattern peculiar to anaesthesia, respectively. Flattened  $P_{O_2}$  peaks following abdominal ventilation were observed only during recovery from anaesthesia. (D) Effects of cooling the bee using an ice pack. (E) Recording from the same animal shown in D, but during rewarming to room temperature. See Table 1 for experimental conditions.

$P_{O_2}$  variation in a bee anaesthetised with chloroform vapour is shown in Fig. 3C. In this bee,  $P_{O_2}$  remained high (8.5–9.2 kPa) even when the bee ceased abdominal ventilation. Until the bee began ventilating at around 5 min, no abdominal movements were observed, although the legs occasionally moved slowly. The  $P_{O_2}$  pattern after abdominal pumping began differed from that in an unanaesthetised bee. When abdominal pumping stopped,  $P_{O_2}$  decreased much more slowly in the anaesthetised bee, giving the  $P_{O_2}$  peaks a plateau. It is possible that the spiracles remain open for this period after abdominal pumping ceases in the anaesthetised bee, although spiracle movements were not observed in this study.

Many authors have proposed that discontinuous ventilation functions to reduce water or heat loss (Hadley and Quinlan, 1993; Lighton et al., 1993). Therefore, it was of interest to determine how temperature and humidity affect the pattern of muscle  $P_{O_2}$ . Fig. 3D,E shows the effects of cooling and subsequent rewarming on the pattern of muscle  $P_{O_2}$  variation. Placing an ice pack approximately 2 cm beneath the bee at the onset of the recording shown in Fig. 3D caused the  $P_{O_2}$  cycle to increase in amplitude. This effect was observed in six out of six experiments from three animals. The pattern shown at

the end of Fig. 3D continued for a further 15 min. It was clear that the bee was not cryo-anaesthetised by the cooling procedure because it could still beat its wings (data not shown). The ice pack was removed at the onset of the recording shown in Fig. 3E and the rhythmic  $P_{O_2}$  cycle disappeared (note the different time scale in Fig. 3E). From the present results, we cannot determine whether the cooling or dehydrating effect of the ice pack had the greater effect on the  $P_{O_2}$  pattern.

#### Paralysis measurements

As described above,  $P_{O_2}$  in the bee decreased between periods of abdominal pumping. A spatial profile of  $P_{O_2}$  within the muscle was recorded in resting bees in preliminary experiments; however, consistent results could not be obtained because of large temporal variations in  $P_{O_2}$ . To assess how  $P_{O_2}$  varies spatially within the muscle, the bee was paralyzed with an injection of tetrodotoxin into the haemolymph. This procedure prevented abdominal pumping, and the oxygen supply to the muscle was therefore by diffusion alone. The  $P_{O_2}$  profile was determined by inserting the oxygen electrode into the thorax in 20  $\mu\text{m}$  increments (Fig. 5). The  $P_{O_2}$  profile showed a gradual decrease as depth increased; superimposed on this decrease were

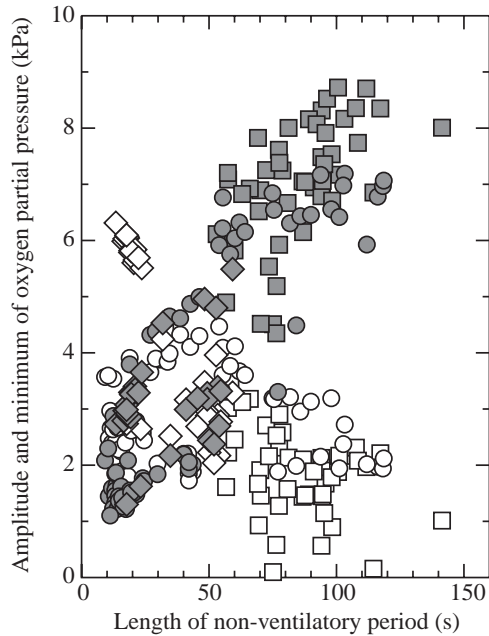


Fig. 4. Effects of non-ventilatory period on flight muscle  $P_{O_2}$  fluctuation amplitude (filled symbols) and minimum value (open symbols) for three different experiments (squares, run 1; circles, run 4; diamonds, run 5; experimental condition are listed in Table 1). Correlation coefficients ( $r$ ) between amplitude and period are 0.373, 0.824 and 0.356 (all  $P < 0.01$ ) and between minimum  $P_{O_2}$  and period are  $-0.517$  ( $P < 0.01$ ),  $-0.061$  (not significant) and  $-0.863$  ( $P < 0.01$ ) for run 1 ( $N=49$ ), run 4 ( $N=80$ ) and run 5 ( $N=33$ ), respectively.

large, acute fluctuations. Muscle fibres in the dorsal longitudinal muscle were elliptical, measuring  $38.2 \pm 6.3 \mu\text{m} \times 55.1 \pm 10.1 \mu\text{m}$  in transverse section ( $N=445$  from four animals; mean  $\pm$  s.d.), among which tracheae  $13.5 \pm 2.8 \mu\text{m}$  in diameter were located  $46.6 \pm 8.8 \mu\text{m}$  apart ( $N=16$  from one animal). Tracheoles tapering to less than  $1 \mu\text{m}$  in diameter penetrated into each of the muscle fibres after bifurcating from the surrounding tracheae. The tracheae among the muscle fibres ran in all directions. It is likely that  $P_{O_2}$  is uniformly high outside the muscle fibres and decreases rapidly towards the centre of each muscle fibre, thus producing the sharp  $P_{O_2}$  peaks seen in Fig. 5.

Fig. 6 is a histogram of the distance between the local peaks in the vertical  $P_{O_2}$  profiles. The interpeak distance of  $60\text{--}80 \mu\text{m}$  is similar to the muscle fibre diameter. Scatter within the histogram may be caused by the electrode path crossing the fibre axis at different angles or puncturing the fibre off centre.

#### Flight measurements

$P_{O_2}$  variation in a flight muscle was measured at four different muscle depths in a single bee (Fig. 7). Steady-state conditions during flight could not be achieved because the bee beat its wings for a maximum period of only 15 s. However, two points should be noted. First, flight did not always result in a decrease in  $P_{O_2}$  but instead caused it to approach asymptotically the mean value of  $6.36 \pm 1.83$  kPa. While  $P_{O_2}$  decreased from the onset of the flight in Fig. 7A (e.g. from 8.25

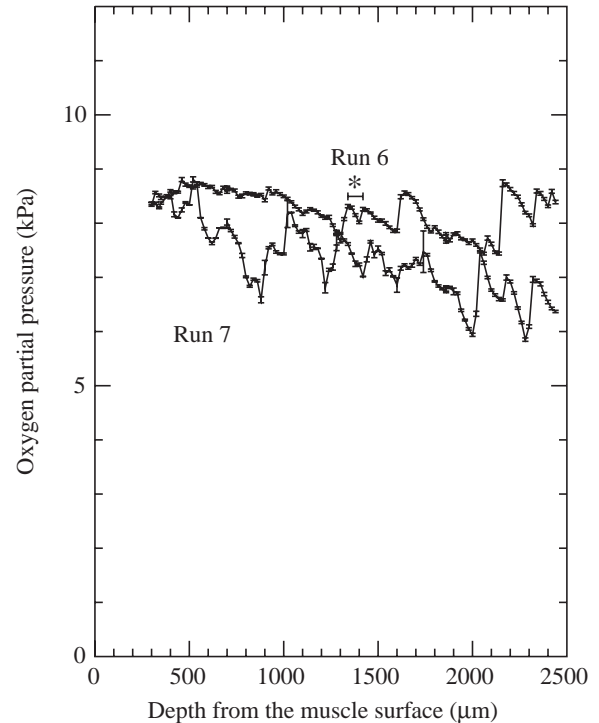


Fig. 5. Vertical  $P_{O_2}$  profile in the dorsal longitudinal muscle of two tetrodotoxin-paralyzed bees. Visible movements were not observed during measurements.  $P_{O_2}$  values were averaged over 15 s. Error bars show  $\pm$  s.d. The asterisk identifies one example of the distance between two maxima.

to 5.85 kPa in the first flight shown), in other flights  $P_{O_2}$  increased (e.g. from 1.20 to 3.22 kPa for the flight ending at 0:58 min in Fig. 7B) or remained unchanged (e.g. from 5.77 to 5.63 kPa for the flight ending at 0:43 min in Fig. 7D). The most common pattern was a decrease in muscle  $P_{O_2}$  at the onset of flight because the bee usually preceded a period of flight by elevating flight muscle  $P_{O_2}$  using abdominal pumping. Second, mean  $P_{O_2}$  during flight was higher than mean resting  $P_{O_2}$  (Table 2). The bee continuously contracted and expanded its abdomen during tethered flight. After flight movements ceased, the  $P_{O_2}$  cycle gradually returned to the regular large-amplitude resting pattern (e.g. Fig. 7A).

Table 2. Oxygen partial pressure in the dorsal longitudinal muscle of the bumblebee during rest, paralysis and flight

Condition	$P_{O_2}$ (kPa)	$N$
Rest 1	$4.49 \pm 1.70$	9
Rest 2	$8.92 \pm 4.79^*$	3
Paralysis	$6.34 \pm 4.46$	12
Flight	$6.36 \pm 1.83^*$	9

Values are means  $\pm$  s.d.

Rest 1, rest during which large-amplitude fluctuations in  $P_{O_2}$  were observed (e.g. Fig. 3A); rest 2, rest during which small-amplitude fluctuations in  $P_{O_2}$  were observed (e.g. Fig. 3B).

\*Significant difference from rest 1 ( $t$ -test,  $P < 0.05$ ).

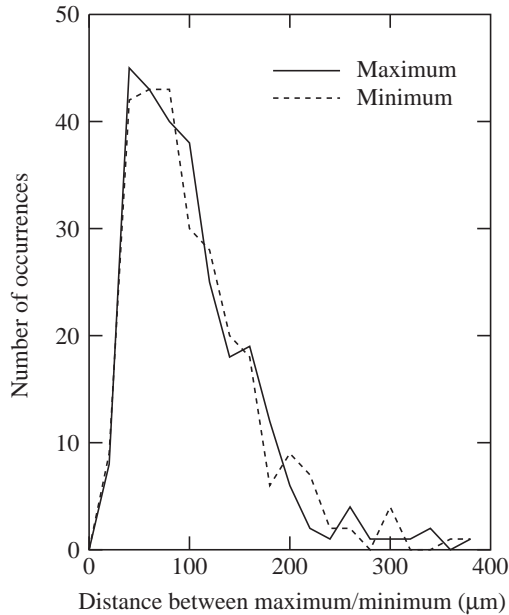


Fig. 6. Histogram of the distance between  $P_{O_2}$  peaks (maximum) and troughs (minimum) found in the vertical  $P_{O_2}$  profiles of the dorsal longitudinal muscle. See Fig. 5 for a definition of the distance measured. Results are from 25 animals.

#### Comparison of mean $P_{O_2}$ among experimental conditions

Mean muscle  $P_{O_2}$  is summarized in Table 2. Resting values were divided into two groups, depending on whether the bee exhibited large- or small-amplitude  $P_{O_2}$  fluctuations and according to whether  $P_{O_2}$  amplitude was greater than 60% of maximum  $P_{O_2}$  or less than 40%. Resting values were used only when the bee did not change its ventilation pattern, move its legs or beat its wings for 15 min.  $P_{O_2}$  amplitudes of 40–60% of maximum  $P_{O_2}$  were observed only rarely (four out of 37 recordings). Flight values were used when the bee beat its wings for periods greater than 5 s (mean  $13.3 \pm 9.7$  s).  $P_{O_2}$  during the last 2 s of 2–11 flights was averaged for each animal.

The mean  $P_{O_2}$  was highest for the small-amplitude resting category, and  $P_{O_2}$  in the large-amplitude category was the lowest among the four conditions. Changes in oxygen consumption caused by flight or by paralysis also affected  $P_{O_2}$ .

Fig. 7. Variation in muscle  $P_{O_2}$  during tethered flight. Bold lines correspond to periods of wing movement similar to flight; broken lines correspond to other movements of the legs or opening and closing of the wings. Traces are from a single bee with the oxygen electrode inserted into the thorax at different depths: (A) 500  $\mu\text{m}$ ; (B) 1000  $\mu\text{m}$ ; (C) 1500  $\mu\text{m}$ ; (D) 2000  $\mu\text{m}$ . See Table 1 for experimental conditions.

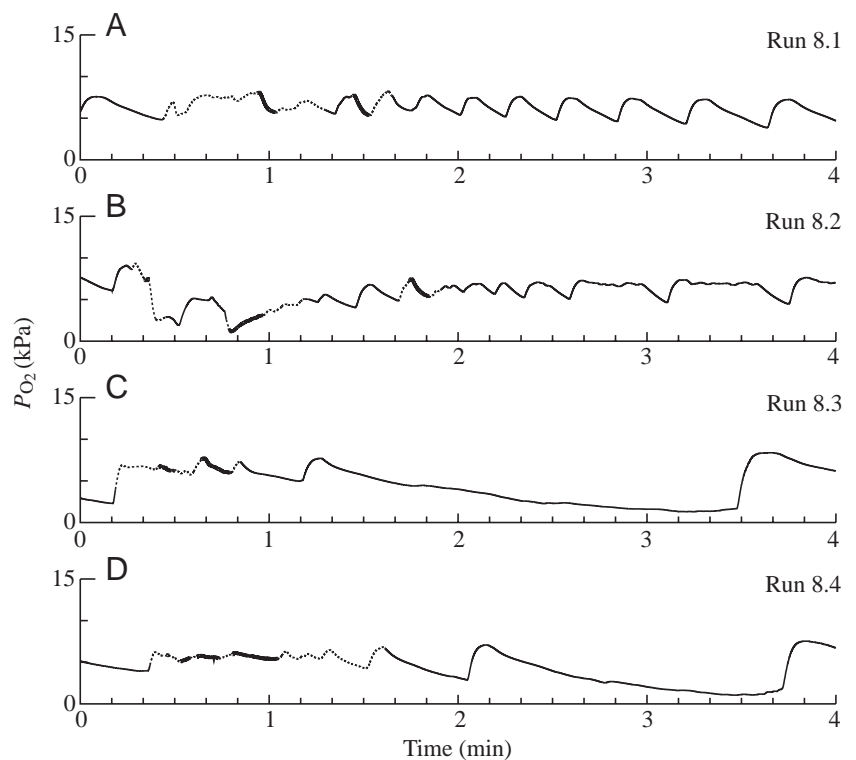
## Discussion

### Oxygen consumption

Bees appear to use convective ventilation for gas exchange during rest and flight and exhibit abdominal pumping for approximately 11% of a ventilation cycle. Ventilation was continuous during tethered flight, so the volume of air inspired will increase approximately 10-fold. If we assume that the oxygen concentration in the expired air does not differ between rest and flight, a flying bee must consume 10 times as much oxygen as a resting bee. Kammer and Heinrich (Kammer and Heinrich, 1974) measured the oxygen consumption of the bumblebee *Bombus vosnesenskii* under various conditions and showed that the oxygen consumption of a flying bee was 42–50 times greater than that of a resting bee at a thoracic temperature of 25 °C. They found an approximately twofold increase in oxygen consumption for every 5 °C increase in thoracic temperature in resting bees. This suggests that the oxygen consumption during tethered flight in the present study was 17–30 times that during rest at a thoracic temperature of 28.5–31.5 °C. These estimates suggest that the efficiency of gas exchange is higher during flight than in a resting bee because oxygen consumption increases more than 17-fold while the volume of inspired air increased only 10-fold. In resting bees, muscle  $P_{O_2}$  changed substantially during ventilation, so the efficiency of oxygen exchange will also have varied over time because this efficiency is proportional to the  $P_{O_2}$  difference between the inspired air and the tissues.

### Effects of thoracic temperature

The sensitivity of a polarographic electrode is affected by the temperature of the surrounding medium. The sensitivity of



the electrode used here increases linearly by  $2.8\% \text{ } ^\circ\text{C}^{-1}$  with increasing temperature (Komai, 1998). In preliminary experiments, simultaneous insertion of a thermocouple was found to suppress flight activity, so thoracic temperature was not measured in the present study. However, any effects of temperature may be negligibly small. Room temperature was  $28.5\text{--}31.5\text{ } ^\circ\text{C}$  and was controlled to within  $0.5\text{ } ^\circ\text{C}$  during measurements. Analysis of the non-flight conditions excluded data where the bee moved its legs or wings, so the thoracic temperature should be equilibrated with the ambient temperature during the measurement. Muscle shivering was not observed under non-flight conditions. In the flight experiments, the bees flew briefly 4–5 times over 2–3 min followed by a rest period of 10 min or more before subsequent flights. Thus, heat production during the first set of flights should not affect the subsequent flights. The mean total time spent flying for the 4–5 flights was 34.5 s, and the longest flight lasted 23.9 s. The maximum rate of increase in thoracic temperature during flight that can be calculated from the data of Kammer and Heinrich (Kammer and Heinrich, 1974) is  $2.8\text{ } ^\circ\text{C min}^{-1}$ ; in the hawkmoth, this value is  $3.1\text{ } ^\circ\text{C min}^{-1}$ , and the rate of decrease after a flight is  $2.4\text{ } ^\circ\text{C min}^{-1}$  (Komai, 1998), so the increase in thoracic temperature is likely to be less than  $1.1\text{ } ^\circ\text{C}$  ( $=2.8/60 \times 23.9$ ) in the flight measurements, giving a possible overestimation of  $P_{\text{O}_2}$  of less than 3.3%. The difference in mean  $P_{\text{O}_2}$  between flight and resting with the large-amplitude pattern is statistically significant ( $P < 0.05$ ) even when the temperature change of  $1.1\text{ } ^\circ\text{C}$  is taken into account.

#### Gas transport in resting animals

In Fig. 8, the rate of change in muscle  $P_{\text{O}_2}$  from the onset of ventilation or flight is plotted. Muscle  $P_{\text{O}_2}$  changed asymptotically from the beginning of a series of abdominal contractions, indicating that fresh air is convected close to the muscle fibres by the ventilatory air flow but that diffusion of oxygen into the muscle fibres determines the rate of  $P_{\text{O}_2}$  change. Old air in the tracheal network is rapidly replaced by convection within the first few abdominal contractions, and oxygen then diffuses towards the muscle fibres. At the beginning of a series of abdominal contractions,  $P_{\text{O}_2}$  in the muscle fibres rose steeply because oxygen flux is proportional to the  $P_{\text{O}_2}$  difference between the muscle fibre and the point to which fresh air is convected. As  $P_{\text{O}_2}$  increases in the muscle fibre, the oxygen diffusion gradient gradually decreases. Finally, muscle  $P_{\text{O}_2}$  will reach a plateau when the oxygen supply balances the metabolic rate. The oxygen supply to the muscle is therefore a diffusion-based phenomenon. Abdominal pumping prevents the tracheal  $P_{\text{O}_2}$  from decreasing. The pattern of change in  $P_{\text{O}_2}$  observed here in resting animals is consistent with the above description, although  $P_{\text{O}_2}$  during abdominal contractions did not reach a steady state, suggesting that the bee ceases ventilation when  $P_{\text{O}_2}$  reaches a certain level.

The time required to reach steady state can be used to determine the extent of the diffusion-dominated region around

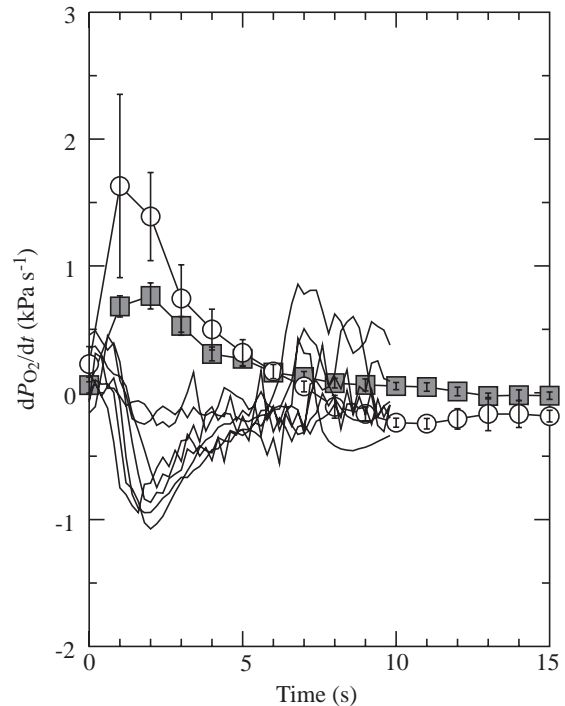


Fig. 8. Rate of change in muscle  $P_{\text{O}_2}$  ( $dP_{\text{O}_2}/dt$ ) relative to the onset of abdominal pumping or flight. Circles indicate run 1 ( $N=7$ ) and squares indicate run 3 ( $N=7$ ). Values are means  $\pm$  s.d. Lines without symbols are for run 8 ( $N=7$ ). The abscissa is relative time from the onset of abdominal pumping for runs 1 and 3, and from the onset of flight for run 8. Experimental conditions are listed in Table 1.

and within the muscle fibre. The time taken ( $\delta t$ ) to diffuse a certain distance ( $\delta l$ ) is given by the equation:

$$\delta l \approx \sqrt{D\delta t}, \quad (3)$$

where  $D$  is diffusivity; for oxygen in water,  $D=2.5 \times 10^{-5} \text{ cm}^2 \text{ s}^{-1}$ . If we take  $\delta t$  as 6–10 s (i.e. where the change in muscle  $P_{\text{O}_2}$  returns to zero in Fig. 8), the distance  $\delta l$  is 120–160  $\mu\text{m}$ . The muscle fibre is an ellipse measuring  $38.2 \pm 6.3 \mu\text{m} \times 55.1 \pm 10.1 \mu\text{m}$  in transverse section, and the surrounding tracheae are distributed  $46.6 \pm 8.8 \mu\text{m}$  apart. The calculated distance  $\delta l$  is therefore similar to, although slightly larger than, the expected diffusion distance based on the muscle structure. This may suggest that fresh air does not flow all the way to the muscle fibre during abdominal pumping. However, analysis is difficult without precise geometrical information because the muscle is heterogeneous, and diffusivities in the cytoplasm and across the tracheole wall, which may be a barrier to gas transport, are not known. The resting bumblebee therefore uses convective gas transport for bulk movement of air into the tracheal system, but the final step in gas exchange is diffusion-limited.

#### Gas transport during flight

At the onset of flight, muscle  $P_{\text{O}_2}$  began to change immediately, irrespective of the direction of this change. The rate of oxygen consumption increases dramatically at the

initiation of flight (17-fold or more), so the oxygen levels immediately surrounding a muscle fibre will be reduced as the oxygen is consumed by mitochondria. Oxygen will diffuse from the tracheole into the muscle fibre according to the  $P_{O_2}$  gradient thus established. An initial reduction in  $P_{O_2}$  should, therefore, occur in the flight muscle of the bumblebee as the  $P_{O_2}$  gradient becomes established; however, this was not observed during measurements (some of the lines for flight are positive in the first second in Fig. 8), implying that it may be too rapid or too small to detect using the present methods. In other words, muscle  $P_{O_2}$  decreases until fresh air reaches the muscle fibres.

To interpret these results, gas transport phenomena must be considered. Because the tracheole is blind-ending, the concentration field near the muscle fibre is dominated by diffusive gas transport. The absence of an initial reduction in  $P_{O_2}$  levels on flight initiation in the present recordings suggests that it occurs in less than 0.1 s. In the muscle fibre, a period of less than 0.1 s implies that the mitochondria are located close to the tracheoles. The exact period will depend on the time taken to develop the concentration gradient between the mitochondrion and the tracheole. For oxygen flux into the muscle fibre to increase within 0.1 s, it can be estimated from equation 3 that the diffusion distance must be less than 1.5  $\mu\text{m}$  between the mitochondrion and the tracheole ( $D=2.5 \times 10^{-5} \text{ cm}^2 \text{ s}^{-1}$ ). In addition, the value 0.1 s suggests that the bee can create and utilise ventilatory flow to the immediate vicinity of the muscle fibre. If unidirectional flow occurs from the abdominal air sac to the thoracic air sac, an initial reduction in  $P_{O_2}$  should have been detected because it must take longer than 0.1 s for oxygen to diffuse from a thoracic air sac to a tracheole through the trachea ( $\delta l=2\text{--}3 \text{ mm}$ ,  $D=0.21 \text{ cm}^2 \text{ s}^{-1}$ ). However, such flow has not been shown to exist; no specific tracheal structures have been identified that would allow unidirectional flow.

From Fig. 8, approximately 10 s was required for  $dP_{O_2}/dt$  to reach zero, although fresh air reached the immediate vicinity of the muscle fibre just after flight initiation. Diffusion in the muscle fibre determines the time to reach a steady-state  $P_{O_2}$  during flight; it is not determined by diffusion from the tracheole to the mitochondrion but by diffusion from the tracheoles to the centre of the muscle fibre. In principal, the time to reach the steady state is the same as in the resting bee.

#### *Control of the respiratory system*

Alterations to ventilatory behaviour at the onset of locomotion are common in vertebrates and invertebrates. Ramirez and Pearson (Ramirez and Pearson, 1989) recorded electromyograms from the flight muscle and the respiratory muscle, and action potentials from the neurons, in a locust, *Locusta migratoria*, and identified an interneurone that linked flight to respiration. This interneurone, which controls the initiation of flight, resets the respiratory system at the onset of flight; respiration ceases for several seconds and then restarts with an elevated ventilation frequency. These findings indicate that the locust respiratory system is controlled by a feedforward mechanism at the initiation of flight.

The present results imply that a feedforward mechanism also controls respiratory behaviour during bumblebee flight. If a feedback mechanism were involved, a time lag should exist. In a feedback mechanism, controlling factors such as oxygen shortage, carbon dioxide excess and the presence of humoral agents must be detected by appropriate receptors in the flight muscle before respiratory behaviour can be altered. However, muscle  $P_{O_2}$  did not always decrease at the onset of flight, and the ventilatory frequency changed simultaneously with the onset of flight.

An increase in respiration rate after exercise is commonly observed in insects, and factors such as tracheal  $P_{O_2}$  and  $P_{CO_2}$  and haemolymph pH are considered to be responsible. Krolikowski and Harrison (Krolikowski and Harrison, 1996) measured tracheal ventilatory pressure to evaluate precisely the respiratory rate following locomotion (continuous jumping) in a locust *Melanoplus differentialis*, after injecting acid or base into the haemolymph or replacing the tracheal gas with several gas mixtures. Their results showed that post-exercise respiration rate was not affected by changes in haemolymph pH,  $P_{O_2}$  or  $P_{CO_2}$  or by tracheal  $P_{O_2}$  or  $P_{CO_2}$ . They suggested that a humoral feedback mechanism was possible together with a neuronal feedforward mechanism. In the post-flight bumblebee, the  $P_{O_2}$  cycle usually increased in amplitude to the regular large-amplitude pattern within 1 min of the flight. However, a gradual transition to this pattern lasting longer than 3 min (e.g. Fig. 7A) and cases in which intermittent ventilation directly followed flight were occasionally observed. As can be seen from Fig. 7A, muscle  $P_{O_2}$  could be restored to pre-flight values within 15 s, which is less than the time taken to restore the regular large-amplitude pattern following flight. Thus, tracheal and tracheolar  $P_{O_2}$  will be restored before the  $P_{O_2}$  cycle returns to the pre-flight pattern. This result suggests that humoral metabolites or a neuronal feedforward mechanism control the post-flight  $P_{O_2}$  pattern.

#### *Comparison with the hawkmoth*

In a recent study (Komai, 1998),  $P_{O_2}$  was measured in a hawkmoth *Agrius convolvuli* thorax using the same methods. The resting oxygen demands of the hawkmoth are met by diffusion, so  $P_{O_2}$  is constant in the resting moth. The structure of the flight muscles differs between the bee and the moth, and the spatial  $P_{O_2}$  profile therefore also differs. The dorsal longitudinal muscle of the hawkmoth consists of four layers, each 1000–1500  $\mu\text{m}$  thick. Tracheal trunks lie between the layers; the bifurcated tracheae penetrate the muscle layer. In hawkmoths,  $P_{O_2}$  is highest between the muscle layers, gradually decreasing within a layer with distance from the surface. The  $P_{O_2}$  difference between the inside and outside of the muscle layer is approximately 3 kPa. The  $P_{O_2}$  difference between the outside and inside of a muscle fibre is approximately 0.5 kPa; in the paralysed bumblebee, it is 1.4 kPa.

$P_{O_2}$  variation during flight also differs between the bumblebee and the hawkmoth. In the bumblebee,  $P_{O_2}$  appeared rapidly to approach a constant value (6.36 kPa) after

the onset of flight. In contrast,  $P_{O_2}$  in the hawkmoth dropped rapidly in the first few seconds of flight, then increased and reached a plateau after 2 min. During moth flight, muscle  $P_{O_2}$  was higher than during rest in some cases, indicating that the augmented oxygen supply exceeded the local oxygen demand. The observed differences between these species may be due to differences in their tracheal network and gas transport mechanism. The tracheal network runs uniformly throughout the bumblebee's flight muscle, but that in the hawkmoth is dendric towards the centre of the muscle layers. While the flying bee ventilates in the same way during rest and flight, the moth switches its ventilation mechanism during flight from diffusion to convection. Since the moth does not have air sacs to contract, oxygen supply at rest occurs by diffusion. Without compressible air sacs, the hawkmoth uses deformation of the tracheae by the contracting flight muscles to drive ventilatory air flow during flight. Tidal volume is small in the moth. The ventilatory flow in the bee is a unidirectional periodic flow of large volume and low frequency (approximately 3 Hz); that in the moth is an oscillatory flow of small tidal volume and high frequency (approximately 30 Hz).

The bumblebee and the hawkmoth use different methods of ventilation (abdominal pumping and muscle pumping, respectively), and other large insects can use both ventilation methods. The behaviour of the spiracles of locusts (Miller, 1960), dragonflies (Miller, 1962) and beetles (Miller, 1966) was found to be synchronized with abdominal movements, suggesting unidirectional air flow in the tracheae. Weis-Fogh (Weis-Fogh, 1967) measured the volumetric change in the tracheal network as a function of wing angular position and estimated that the volumetric change was large enough to contribute to gas transport during flight in a locust. The  $P_{O_2}$  variation in the muscles of these insects is unknown, so the degree to which the two ventilation methods contribute to gas exchange is not yet understood.

The design of the tracheal network and the ventilation method should be related to other factors too. For example, the hawkmoth *Agrius convolvuli* remains stationary during the day and flies only at night (Kiguchi and Shimoda, 1994). Furthermore, the adult moth rarely feeds. Respiration by diffusion alone must be economical, and the absence of movements may assist the moth to avoid predation. However, the hawkmoth will be unable to tolerate extended dry periods because the spiracles remain open.

I thank H. Baumgärtl for technical advice on the oxygen microelectrode. The electrode was produced in collaboration with K. Tanishita and K. Oka at Keio University.

## References

- Bailey, L. (1954). The respiratory currents in the tracheal system of the adult honey-bee. *J. Exp. Biol.* **31**, 589–593.
- Baumgärtl, H. (1987). Systematic investigations of needle electrode properties in polarographic measurements of local tissue  $P_{O_2}$ . In *Clinical Oxygen Pressure Measurement* (ed. A. M. Ehrly, J. Hauss and R. Huch), pp. 17–42. London: Springer-Verlag.
- Hadley, N. F. and Quinlan, M. C. (1993). Discontinuous carbon dioxide release in the eastern lubber grasshopper *Romalea guttata* and its effect on respiratory transpiration. *J. Exp. Biol.* **177**, 169–180.
- Kammer, A. E. and Heinrich, B. (1974). Metabolic rates related to muscle activity in bumblebees. *J. Exp. Biol.* **61**, 219–227.
- Kiguchi, K. and Shimoda, M. (1994). The sweet potato hornworm, *Agrius convolvuli*, as a new experimental insect: continuous rearing using artificial diets. *Zool. Sci.* **11**, 143–147.
- Komai, Y. (1998). Augmented respiration in a flying insect. *J. Exp. Biol.* **201**, 2359–2366.
- Krolikowski, K. and Harrison, J. F. (1996). Haemolymph acid–base status, tracheal gas levels and the control of post-exercise ventilation rate in grasshoppers. *J. Exp. Biol.* **199**, 391–399.
- Levy, R. I. and Schneiderman, H. A. (1966). Discontinuous respiration in insects. II. The direct measurement and significance of changes in tracheal gas composition during the respiratory cycle of silkworm pupae. *J. Physiol., Lond.* **12**, 83–104.
- Lighton, J. R. B., Garrigan, D. A., Duncan, F. D. and Johnson, R. A. (1993). Spiracular control of respiratory water loss in female alates of the harvester ant *Pogonomyrmex rogosus*. *J. Exp. Biol.* **179**, 233–244.
- Mill, P. J. (1985). Structure and physiology of the respiratory system. In *Comprehensive Insect Physiology Biochemistry and Pharmacology: Integument, Respiration and Circulation*, vol. 3 (ed. G. A. Kerkut and L. I. Gilbert), pp. 517–593. Oxford: Pergamon Press.
- Miller, P. L. (1960). Respiration in the desert locust. III. Ventilation and the spiracles during flight. *J. Exp. Biol.* **37**, 264–278.
- Miller, P. L. (1962). Spiracle control in adult dragonflies (Odonata). *J. Exp. Biol.* **39**, 513–535.
- Miller, P. L. (1966). The supply of oxygen to the active flight muscles of some large beetles. *J. Exp. Biol.* **45**, 285–304.
- Miller, P. L. (1974). Aerial gas transport. In *The Physiology of Insecta: Respiration*, vol. 6, second edition (ed. M. Rockstein), pp. 345–402. New York: Academic Press.
- Ramirez, J. M. and Pearson, K. G. (1989). Alteration of the respiratory system at the onset of locust flight. I. Abdominal pumping. *J. Exp. Biol.* **142**, 401–424.
- Snodgrass, R. E. (1984). The abdomen. The respiratory system. In *Anatomy of the Honey Bee*, pp. 134–167, 227–242. Ithaca, London: Comstock Publishing Associates.
- Weis-Fogh, T. (1964). Diffusion in wing muscle, the most active tissue known. *J. Exp. Biol.* **41**, 229–256.
- Weis-Fogh, T. (1967). Respiration and tracheal ventilation in locusts and other flying insects. *J. Exp. Biol.* **47**, 561–587.
- Wolf, T. J., Ellington, C. P., Davis, S. and Feltham, M. J. (1996). Validation of the doubly labelled water technique for bumblebees *Bombus terrestris* (L.). *J. Exp. Biol.* **199**, 959–972.